Published online 10 April 2017

Nucleic Acids Research, 2017, Vol. 45, No. 10 ***5901–5912***
doi: 10.1093/nar/gkx261

DICER and ZRF1 contribute to chromatin decondensation during nucleotide excision repair

Shalaka Chitale[1,2] and Holger Richly[1,*]

[1]Laboratory of Molecular Epigenetics, Institute of Molecular Biology (IMB), Ackermannweg 4, 55128 Mainz, Germany and [2]Faculty of Biology, Johannes Gutenberg University, 55099 Mainz, Germany

Received November 28, 2016; Revised March 20, 2017; Editorial Decision April 03, 2017; Accepted April 04, 2017

ABSTRACT

Repair of damaged DNA relies on the recruitment of DNA repair factors in a well orchestrated manner. As a prerequisite, the chromatin needs to be decondensed by chromatin remodelers to allow for binding of repair factors and for DNA repair to occur. Recent studies have implicated members of the SWI/SNF and INO80 families as well as PARP1 in nucleotide excision repair (NER). In this study, we report that the endonuclease DICER is implicated in chromatin decondensation during NER. In response to UV irradiation, DICER is recruited to chromatin in a ZRF1-mediated manner. The H2A–ubiquitin binding protein ZRF1 and DICER together impact on the chromatin conformation via PARP1. Moreover, DICER-mediated chromatin decondensation is independent of its catalytic activity. Taken together, we describe a novel function of DICER at chromatin and its interaction with the ubiquitin signalling cascade during GG-NER.

INTRODUCTION

Nucleotide excision repair (NER) represents a major DNA repair pathway, which removes helix distorting DNA lesions such as 6-4 photoproducts and cyclobutane pyrimidine dimers (CPDs) from chromatin (1). Mammalian NER comprises of two subpathways that vary in the mechanism of DNA lesion recognition. Transcription-coupled NER (TC-NER) is carried out at regions of active transcription, where stalled RNA Polymerase II elicits the DNA damage response. Global genome NER (GG-NER) carries out the transcription-independent repair of DNA lesions. The recognition step of both subpathways is followed by verification of the lesion, and by the generation of the pre-excision complex consisting of TFIIH and its helicase subunits XPB and XPD. Subsequently, the lesion is excised by the endonucleases XPF and XPG and the gap is refilled by DNA polymerases (2,3).

Another important feature of DNA repair and a hallmark of the DNA damage response is H2A-ubiquitylation. Ubiquitin signaling has been extensively studied at DNA double strand breaks. The E3 ligases RNF168, RNF8 and RING1B were reported to catalyze H2A-ubiquitylation thereby facilitating accumulation of repair proteins (4–7). During NER, H2A-ubiquitylation is catalyzed by the E3 ligase RNF8, the UV–DDB-CUL4 and UV–RING1B complexes (8–12). We have recently shown that ZRF1 is an essential factor in NER (12). ZRF1 interacts with the H2A–ubiquitin mark generated by the UV–RING1B complex. Its presence at damaged chromatin depends on XPC, a structure specific DNA binding factor, which specifically binds helix-distorting structures (12–14). At the lesion site, ZRF1 mediates the specific exchange of the cullin and E3 ligase subunits from the UV-RING1B complex, converting it into the DDB–CUL4A E3 ligase complex (12,15). However, it is currently not known whether ZRF1 interacts with other components of chromatin signaling during the DNA damage response.

The endoribonuclease DICER contributes to the DNA damage response by generating small non-coding RNAs that entail the sequence of the damaged locus (16–19). At DNA double strand breaks, DICER seems to be essential for the activation of the DNA damage response and checkpoint control (16). More recently, it was demonstrated that DICER is necessary for the recruitment of the mediators MDC1 and 53BP1 (20). However, insights into the molecular mechanism of DICER at DSBs are still relatively sparse. Apart from its specific regulatory function at DSBs, DICER is involved in the formation of heterochromatin (21). Here, we report that DICER plays an essential role in NER and that, in contrast to its role in gene regulation, it facilitates the decondensation of damaged chromatin.

MATERIALS AND METHODS

Unscheduled DNA synthesis

UDS experiments were performed as described previously (22). Briefly, MRC5 fibroblasts were transfected with siRNAs, serum starved for 24 h, irradiated with UV light (20 J/m^2) and incubated with 10 μM EdU (Thermo Fisher) for 2 h. Alexa-488-azide (Thermo Fisher) was conjugated to EdU using the Click-reaction. The coverslips were mounted

*To whom correspondence should be addressed. Tel: +49 6131 39 21440; Email: h.richly@imb-mainz.de

in Vectashield with DAPI. Images were acquired with the LAS AF software (Leica) using a AF-7000 widefield microscope (Leica) with a 63×/1.4 oil immersion objective and an ORCA CCD camera (Hamamatsu). Images were analyzed using ImageJ. DAPI was used to define nuclei, and EdU intensity within nuclei was measured after background subtraction. 150–300 nuclei were analyzed per sample. Mean intensities of +UV and –UV conditions for all cells were calculated, and used to estimate the DNA repair occurring in the particular sample.

Recovery of RNA synthesis (RRS) assay

RRS assay was performed as described previously (22). Briefly, MRC5 cells were transfected with siRNAs, irradiated with UV light (11 J/m^2), and incubated in DMEM containing 1% FBS for 12 h. This was followed by 2 h incubation with EU (Sigma) and subsequent fixation. Alexa-488-azide (Thermo Fisher) was conjugated to EU using the Click-reaction. The coverslips were mounted in Vectashield with DAPI. Images were acquired with the LAS AF software (Leica) using a AF-7000 widefield microscope (Leica) with a 63×/1.4 oil immersion objective and an ORCA CCD camera (Hamamatsu). Images were analyzed using ImageJ as described (22).

C. elegans culture

Nematodes were cultured on agar plates at 20°C according to standard procedures. Mutant strains were outcrossed at least three times to the wildtype strain (N2) to clear the genetic background prior to analysis. Some strains were provided by the CGC, which is funded by NIH Office of Research Infrastructure Programs (P40 OD010440).

Measuring DNA damage response in the *C. elegans* germ line

The L4 survival assay was carried out as described (23). Briefly, late-L4 larval hermaphrodites were irradiated with different doses of UV light. The damage sensitivity of the meiotic pachytene cells of the germline was measured by determining the survival of embryos produced between 24 and 30 h post L4 stage irradiation.

Measuring DNA damage response in the *C. elegans* soma via developmental arrest

The L1 development arrest assay was carried out as described (23). Briefly, L1 staged worms were synchronized via starvation and irradiated with different doses of UV-C light. Relative larval-stage stalling was determined after 60 h, when control worms were fully fertile.

Cell lines and transfections

HEK293T, U2OS and U2OS 2-6-3 cells were cultured in DMEM supplemented with 10% FBS at 37°C and 5% CO_2. The medium for U2OS 2-6-3 cells was additionally supplemented with 100 μg/ml Hygromycin to maintain stable insertion of the LacO cassette. The HEK293 T-REx cell lines shScrambled (containing non-targeting shRNA; #2800272) and shDICER (containing anti-DICER shRNA; #2800353) were a gift from Petr Svoboda and have been described in (24). Normal skin fibroblasts (GM15876), MRC-5 fibroblasts (AG05965), XP-A patient cells (GM00710) and CS-A patient cells were purchased from the Coriell Cell Repositories and cultured in DMEM, supplemented with 15% FBS.

Transfection of U2OS 2-6-3 and HEK293T cells was performed by Lipofectamine 2000 (Invitrogen) transfection according to manufacturer's instructions. Plasmids used were mCherry-LacR-ZRF1, mCherry-LacR-DICER, mCherry-LacR-DICER^{44ab}, EGFP-LacR and EGFP-LacR-DDB2, FLAG-HA-DICER (Addgene #19881), pCMV2-FLAG-ZRF1. Information on cloning strategies available on request. Control (D-001206-13-05) and DICER (M-003483-00-0005) siRNA was purchased from Dharmacon (siGENOME SMARTpool). Control (EHUEGFP) and PARP1 (EHU050101) esiRNAs were purchased from Sigma.

Plasmid transfection in MRC-5 cells was performed using a Nucleofector 2b (Lonza), Kit:R, program V-020.

UV irradiation and drug treatment

Cells were irradiated with 20 J/m^2 UV-C using a CL-1000 UV-crosslinker (UVP) unless stated otherwise. Micropore irradiation experiments were performed on MRC5 fibroblasts. Cells were exposed to localized UV damage (100 J/m^2) using a micropore membrane with 3-μm pore size as described previously (25).

PARP inhibitor treatment was performed as described in (26). Briefly, 5 mM IPTG was added to the cells before and during transfection with the mCherry-LacR-fusion plasmid. IPTG was washed out 24 h post-transfection, and replaced with medium containing 1 μM PARP inhibitor (KU-0058948). Cells were incubated with inhibitor for 16 h, followed by fixation and staining.

Immunofluorescence

Cells were fixed in 4% PFA for 10 min at room temperature. When indicated, pre-extraction with CSK buffer (10 mM PIPES pH 7.4, 100 mM NaCl, 300 mM sucrose, 3 mM $MgCl_2$) containing 0.2% Triton-X was performed for 5 min on ice prior to fixation. Cells were incubated overnight with primary antibody at 4°C. Subsequently, cells were incubated with Alexa-fluorophore-conjugated secondary antibodies (Life Technologies). The mounting was carried out in Vectashield with DAPI (Vector Laboratories). CPD staining (TDM-2 CosmoBio) was performed according to the manufacturer's protocol, prior to incubation with primary antibodies.

Antibodies

Antibodies used in this study were: anti-DICER (Cell Signaling, #3363), anti-ZRF1 (Novus Biologicals, NBP2-12802). RING1B clone (D22F2, Cell Signaling #5694), XPA (Genetex, GTX103168), H2B (Cell Signaling V119 #8135).

Chromatin association assays

HEK293T cells (unless stated otherwise) were irradiated with UV and crosslinked by formaldehyde at the indicated time points after UV irradiation. Assays were essentially performed as published (27).

Mass spectrometry

Mass-spectrometry sample preparation, measurement and database search were performed as described elsewhere (28). Gradient lengths of 45 or 105 min were chosen depending on the IP material obtained. Raw files were processed with MaxQuant (version 1.5.2.8) and searched against the *Homo sapiens* Uniprot database (25 February 2012) using the Andromeda search engine integrated into MaxQuant and default settings were applied. Proteins with at least two peptides, one of them unique, count as identified.

FLAG purifications

Cells were UV irradiated (20 J/m^2) and harvested 1 h after exposure (unless stated otherwise). FLAG affinity purifications were performed using FLAG-M2 agarose beads as already published (27).

RNAseA digestion

RNAse digestion was performed based on protocols described in (29,30). Briefly, cells were permeabilized in CSK buffer (10 mM PIPES pH 7.4, 100 mM NaCl, 300 mM sucrose, 3 mM $MgCl_2$) containing 0.5% Triton-X and protease inhibitors for 2 min. This was followed by treatment with 1 mg/ml RNAse at RT for 10 min. Cells were then washed once in PBS followed by formaldehyde fixation (for chromatin association assays) or PFA fixation (for immunofluorescence experiments).

MNase digestion and assessment of chromatin condensation

Micrococcal nuclease was obtained from New England Biolabs. MNase digestion was performed as described in (31) with certain modifications. Cells were harvested at specified time points after UV treatment and washed once with Permeabilization Solution I (150 mM sucrose, 80 mM KCl, 35 mM HEPES, pH 7.4, 5 mM K_2HPO_4, 5 M $MMgCl_2$, 0.5 mM $CaCl_2$). Cells were permeabilized in Permeabilization Solution I containing 0.2% Triton X-100 for 2 min. Cells were resuspended in 1 ml Permeabilization Solution II (150 mM sucrose, 50 mM Tris–HCl, pH 7.5, 50 mM NaCl, 2 mM $CaCl_2$) containing 7.5 or 15 units of MNAse and incubated for 5 min at RT. This was followed by cell lysis with TNES (10 mM Tris–HCl, pH 7.4, 0.1 M NaCl, 1 mM EDTA, 1% SDS), RNAse A treatment and Proteinase-K digestion as described. DNA was purified using a Qiaquick PCR purification kit and loaded on a 1.5% Agarose gel. DNA bands were labeled 1–8 from high to low molecular weight. Band intensity was measured using ImageLab (BioRad). Intensities were normalized to the band of highest intensity for each sample, and a graph of relative band intensity versus band number was plotted.

RESULTS

DICER is required for nucleotide excision repair and is recruited to DNA damage sites

DICER has been previously implicated in DNA damage pathways and is thought to play a role in preventing DNA damage by maintaining heterochromatin structure (32,33) as well as indirectly through microRNA mediated regulation of DNA damage checkpoints (34–36). Specifically, it was shown that knockdown of DICER results in miRNA dependent hypersensitivity to UV irradiation (37). In order to differentiate between more global effects of DICER on DNA damage repair and a potentially more specific role in nucleotide excision repair, we performed unscheduled DNA synthesis (UDS) assays. We analyzed EdU incorporation specifically in non-S phase MRC-5 fibroblasts exposed to UV damage. Under these conditions the EdU incorporation reflects the efficiency of the core DNA repair process. As a reference we addressed UDS in XP-A and CS-A patient fibroblasts (Figure 1A). We observed about a 40% decrease of EdU incorporation in DICER knockdown cells as compared to control cells (Figure 1A). This finding suggested that DICER is required for nucleotide excision repair. Next, we wanted to elucidate whether DICER plays a role in either the GG-NER or the TC-NER subpathway. To this end, we monitored the recovery of RNA synthesis (RRS) after exposure to UV damage. Cells deficient specifically in TC-NER (XP-A and CS-A patient fibroblasts) show an impaired recovery, while depletion of GG-NER proteins does not affect the recovery of RNA synthesis. We observed that DICER knockdown cells showed no impairment of RNA synthesis. In contrast XP-A and CS-A deficient fibroblasts showed impaired RRS. (Supplementary Figure S1A). Additionally, we performed survival assays in *C. elegans*. In *C. elegans*, DNA repair in the germ line occurs mainly via GG-NER during early development, while TC-NER is the main NER subpathway employed during larval development (38). Upon UV treatment of a DICER mutant (*dcr-1*), we observed a substantial decrease in egg hatching comparable to that observed in a XPA deficient strain (*xpa-1*), which is essential for survival following UV treatment (39) (Supplementary Figure S1B). In contrast, upon irradiation of L1 larvae, we observed no significant developmental arrest in the DICER mutant (Supplementary Figure S1C). However, we observed a developmental arrest in both XPA (*xpa-1*) and CSB (*csb-1*) deficient worms, which are deficient in total NER and TC-NER, respectively (Supplementary Figure S1C). Taken together these data imply that DICER plays a more prominent role in GG-NER.

Next, we wanted to determine if DICER is recruited to chromatin after UV irradiation. To this end we performed chromatin association assays in HEK293T cells treated with either control or DICER siRNAs followed by UV irradiation (Figure 1B, Supplementary Figure S1D). We found that DICER is specifically recruited to chromatin after UV irradiation. Additionally, to verify if DICER is localized to the site of DNA damage we performed micropore irradiation experiments. Normal fibroblasts were irradiated through a micropore to generate localized damage, and then stained with CPD and DICER antibodies (Figure 1C). We

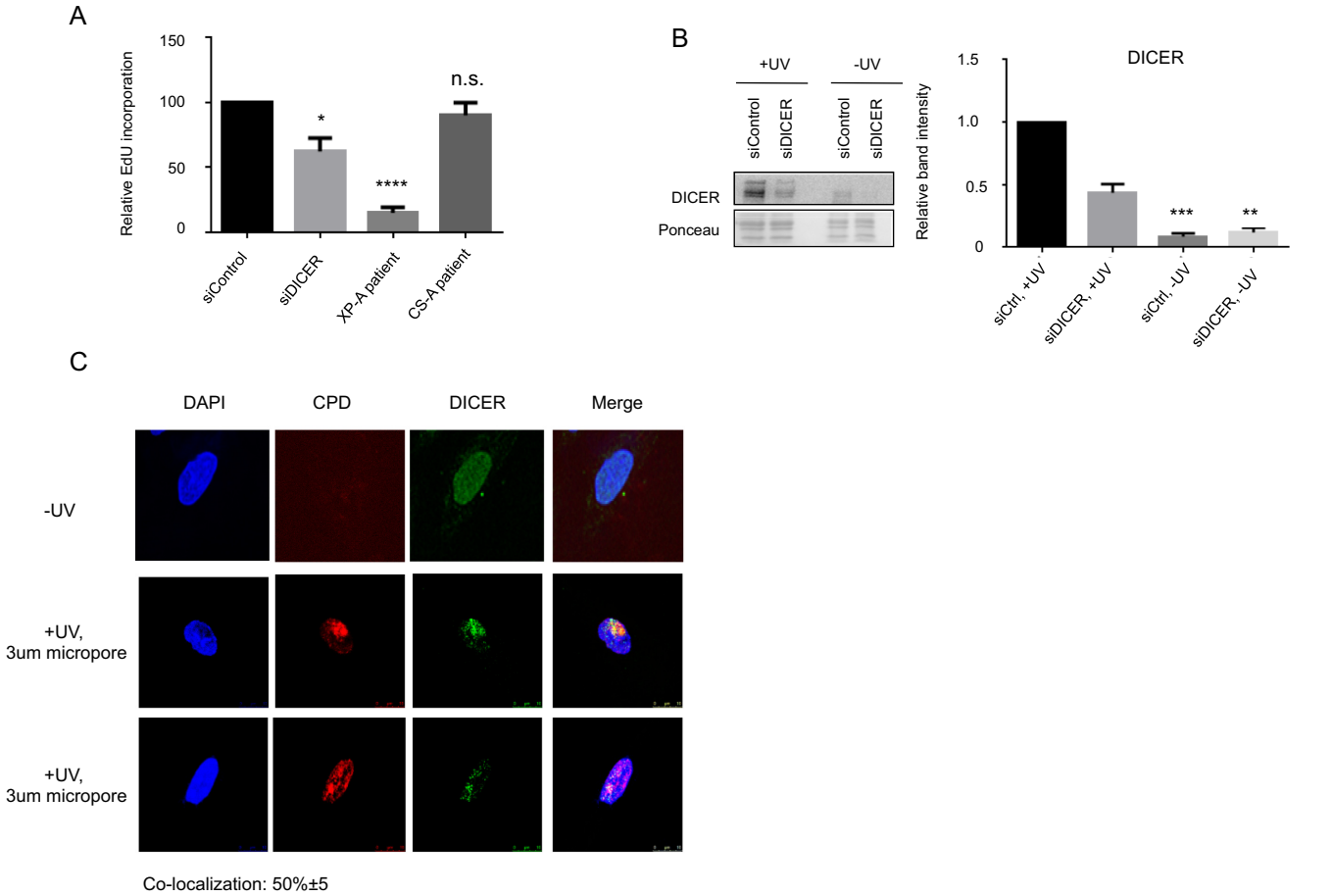

Figure 1. DICER is essential for nucleotide excision repair. (**A**) Knockdown of DICER results in impaired NER. The graph shows relative EdU incorporation as a measure of unscheduled DNA synthesis (UDS) in control (siControl), DICER knockdown (siDICER), XP-A patient fibroblasts (XP-A patient) and CS-A patient fibroblasts (CS-A patient) cells. Mean ± SD, $n = 3$. Statistical significance was assessed by an unpaired t-test. (**B**) DICER is recruited to chromatin after UV damage. (Left panel) The blot shows DICER levels in the chromatin fraction in control (siControl) and DICER knockdown (siDICER) cells in UV unexposed cells and 1 h after UV exposure. (Right panel) Quantification of B. The graph shows the relative band intensities for DICER, normalized to a loading control (Ponceau) for control and DICER knockdown cells in –/+UV conditions. (**C**) DICER is recruited to UV lesions. Immunofluorescence images showing DICER recruitment to DNA lesions (marked by CPD) in cells subjected to irradiation through a 3 μm micropore. Recruitment was observed at 50% ±5 lesions, quantified from 30 cells each. $N = 2$

observed that DICER was recruited to the DNA damage locus in ∼50% of the lesions. These data together suggest that DICER represents an essential factor in nucleotide excision repair in human cells and in *C. elegans*.

DICER interacts with ZRF1 and its recruitment to chromatin is dependent on ZRF1

In order to further investigate the function of DICER in NER, we expressed FLAG tagged DICER in HEK293T cells and performed immunoprecipitations followed by mass spectroscopy (Supplemental Table S1). We observed that DICER interacts strongly with ZRF1. We further confirmed this interaction by immunoblotting the aforementioned immunoprecipitated material (Figure 2A and B). The interaction of the two proteins was recapitulated in reverse immunoprecipitation experiments using FLAG tagged ZRF1 as well (Supplementary Figure S2A). We additionally assessed the nuclear distribution of chromatin bound ZRF1 and DICER in both UV unexposed and UV exposed cells. We found that DICER co-localized with ZRF1 foci at chromatin after UV damage, further confirming the interaction of the two proteins (Supplementary Figure S2B). Next, we assessed the functional interplay of DICER, ZRF1 and the E3 ligase RING1B, which is essential for ZRF1 recruitment to the damage site (12). To this end, we transfected HEK293T cells and HEK293T cell lines expressing short hairpin RNAs (shRNAs) targeting RING1B and ZRF1 with control or DICER siRNA pools followed by UV irradiation (Figure 2C). We observed that knockdown of both ZRF1 and RING1B had an adverse effect on recruitment of DICER to chromatin. These data suggest that RING1B dependent mono-ubiquitylation of H2A and hence tethering of ZRF1 are a prerequisite for DICER recruitment to chromatin. In contrast, siRNA mediated knockdown of DICER did not affect recruitment of RING1B or ZRF1 (Figure 2C, Supplementary Figure S2D), suggesting that DICER probably plays a role downstream of ZRF1.

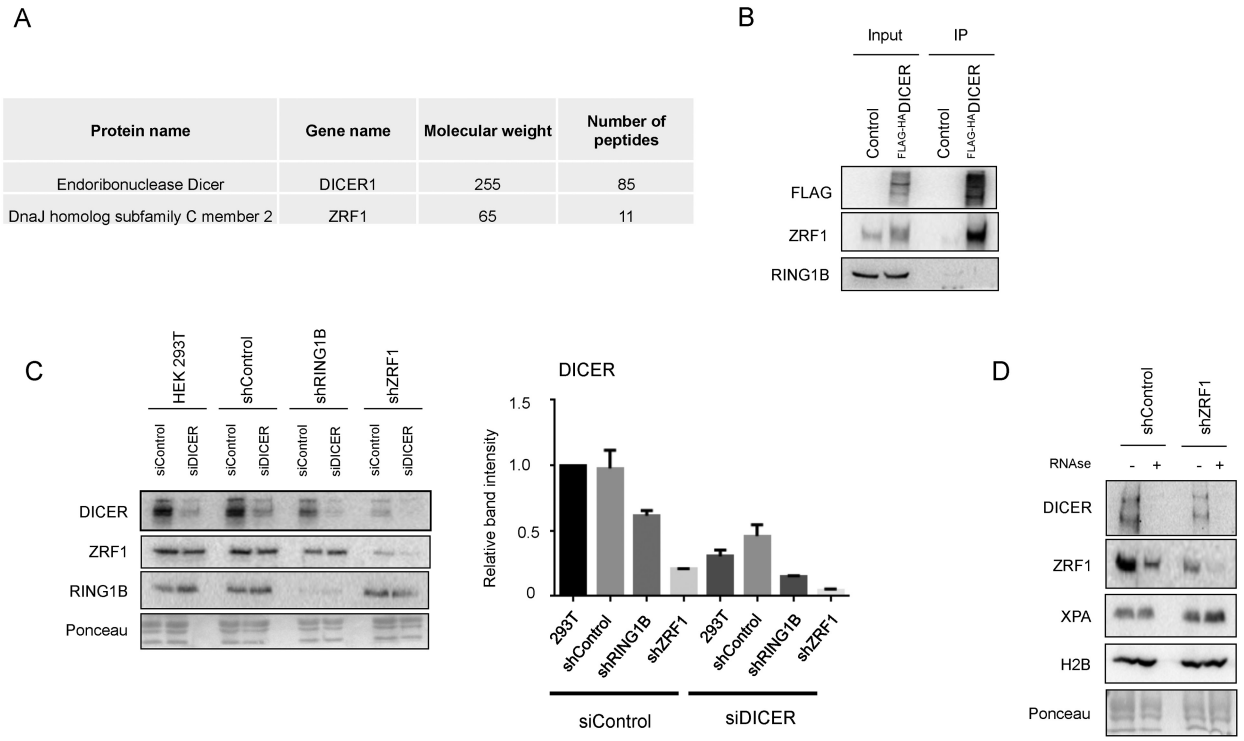

Figure 2. DICER interacts with ZRF1 and is recruited to chromatin in a ZRF1 dependent manner. (**A**) $^{FLAG\text{-}HA}$DICER along with its interactors, was purified from HEK293T cells and the purified material was subjected to mass spectrometry. Strong interaction was seen with ZRF1. The table shows the number of peptides identified by mass spectroscopy for DICER and ZRF1. (**B**) Western blot showing co-immunoprecipitation of ZRF1 in a $^{FLAG\text{-}HA}$DICER purification. (**C**) (Left panel) The blot shows levels of the indicated proteins in chromatin fractions from cells 1 h post UV exposure. Control and DICER siRNA was transfected into the indicated stable shRNA knockdown cell lines. (Right panel) Quantification of C. The graph shows the relative band intensities for DICER, normalized to a loading control (Ponceau) for control and DICER knockdown cells in the indicated knockdown cell lines in –/+UV conditions. (**D**) RNAse treatment leads to loss of DICER and ZRF1 from chromatin. The blot shows levels of the indicated proteins in the chromatin fraction from cells subjected to RNAse treatment.

DICER and ZRF1 interactions with chromatin are RNA dependent

DICER contributes to the generation of heterochromatin and it is known to bind and process RNA (16,17,40). Hence, we next examined whether the association of DICER with chromatin observed after UV irradiation was mediated by RNA. To this end, we irradiated HEK293T cell lines (shControl and shZRF1), permeabilized them and subsequently treated them with RNAseA, prior to cross-linking and chromatin purification (Figure 2D). Upon RNAseA treatment, DICER was completely lost from the chromatin fraction whereas ZRF1 levels at chromatin were dramatically reduced in control cells. Next, we assessed the levels of XPA, a core NER protein involved in damage verification. XPA levels at chromatin were unaffected upon RNAse digestion (Figure 2D). Similarly, we assessed the chromatin bound levels of ZRF1 and DICER by immunofluorescence in presence and absence of RNAseA. We found that RNAse treatment completely disrupted the previously observed foci of ZRF1 and DICER in UV exposed cells (Supplementary Figure S2B and C). These data suggest that DICER and ZRF1 association with chromatin is dependent on RNA.

Considering the RNA dependent association of both DICER and ZRF1 with chromatin, we further examined whether their interaction with each other, is also RNA dependent. To this end, we immunoprecipitated FLAG-tagged DICER and ZRF1, and subsequently incubated the beads in presence or absence of RNAseA. We did not observe a significant change in the ZRF1-DICER interaction upon RNAseA treatment (Supplementary Figure S2D). We additionally performed a SILAC experiment involving a selective degradation of dsRNA and ssRNA species to quantitatively determine the effect of RNAseA treatment on DICER-ZRF1 interaction. We found no dependence of the DICER–ZRF1 interaction on RNA (data not shown). Collectively, these data suggest that DICER and ZRF1 are associated with chromatin in a RNA dependent fashion.

DICER and ZRF1 are required for chromatin decondensation after UV damage

We next addressed the potential functions of DICER and ZRF1 in NER. DICER is known to play a role in establishing heterochromatin by processing small RNAs that maintain a condensed chromatin configuration (40). ZRF1 mediates remodeling of multiprotein complexes at chromatin (12,15,41) and might interact with chromatin remodeling complexes (15). Thus, we hypothesized that DICER and ZRF1 might impact on the chromatin conformation. We additionally performed a purification of FLAG tagged ZRF1, followed by mass spectroscopy to identify its in-

teractors. Upon examining the interactors of both ZRF1 and DICER, we found several chromatin remodelers (Figure 3A and B). Notably, a strong interactor of both ZRF1 and DICER was PARP1, which is known to play a role in chromatin decondensation during NER (42). The *Access-Prime-Repair* model of DNA damage repair suggests that chromatin decondensation precedes DNA repair and is required for access of the repair machinery to the lesion site. We therefore performed MNAse assays to determine the chromatin conformation in both unexposed cells and 1 h after UV irradiation. Knockdown of ZRF1 did not show a significant effect on chromatin structure in unexposed cells (Figure 3C and D). In agreement with the known role of DICER in heterochromatin maintenance, we observed that chromatin from unexposed shDICER cells was more efficiently digested by MNAse than chromatin from control cells (shScrambled) indicated by higher levels of DNA of lower molecular weight (Figure 3E and F). In contrast, upon exposure to UV, we noticed an increase in DNA of high molecular weight in both ZRF1 and DICER knockdown cells (Figure 3C–F, Supplementary Figure S3A–D). This is reflective of a more condensed chromatin state. The chromatin condensation observed in ZRF1 knockdown cells is concurrent with our earlier observation that ZRF1 is required for eviction of RING1B from chromatin (27). Prolonged binding of RING1B causes elevated H2A–ubiquitin levels, which are also a marker for condensed chromatin. Thus, also given the physical interaction of DICER and ZRF1 we speculate that both together are required for efficient de-compaction of chromatin after UV exposure.

In order to determine whether the effect on chromatin decondensation is direct or indirect, we made use of a LacO tethering system in U2OS 2-6-3 cells (43) to directly examine the effect of ZRF1 or DICER tethering to a chromatin array. The LacO array in 2-6-3 cells is known to be heterochromatinized under normal conditions, and the size of the array is used as a common marker for the state of condensation/de-condensation of the chromatin array (43). We found that tethering of ZRF1 led to an increase in the array size compared to the mCherry-LacR tethered control array (Figure 4A and B). Similarly, tethering of DICER also led to an increase in size of the chromatin array (Figure 4A and B). Interestingly, DICER had an even stronger effect on array size than ZRF1 alone. This might suggest that the ZRF1-mediated decondensation occurs potentially by function of DICER. In order to further dissect the role of DICER and ZRF1 in regulating array size, we tethered ZRF1–LacR to the array in control and DICER knockdown cells. We found that knockdown of DICER reduced the ZRF1 dependent increase in array size (Figure 4C). However, co-tethering of ZRF1 and DICER did not further increase the size of the array as compared to tethering of DICER alone (Supplementary Figure S4A). These data together suggest that DICER and ZRF1 are potentially involved in chromatin decondensation via similar mechanisms, and that ZRF1 acts in a DICER dependent manner.

DICER has been described to play a role in the establishment of heterochromatin via processing of small RNAs (44). Recently, it was also shown that DICER contributes to acetylation of histones via small RNA mediated recruitment of TIP60 (45). Hence, we wanted to determine whether the effect of DICER on chromatin decondensation was also dependent on the RNA processing activity of DICER. Thus, we generated a completely inactive DICER mutant (DICER^{44ab}) (46). We tethered DICER^{44ab} –LacR to chromatin, and analyzed the array size as a measure of chromatin decondensation (Figure 4A and D). Surprisingly, we found that the array size was similar when tethering either wildtype or mutant DICER. Thus, it seems that the potential role of DICER in chromatin decondensation is unrelated to its ribonuclease activity.

In order to confirm these findings, we compared the activity of wildtype and mutant DICER on chromatin in UV exposed cells. We expressed either mCherry-DICER or mCherry- DICER^{44ab} in shDICER cells (Supplementary Figure S4B) and then performed an MNase assay on unexposed cells and and after UV exposure. We found that expression of wildtype DICER was able to reverse the overall decondensation of chromatin observed in unexposed DICER knockdown cells (Figures 3F and 4E). In contrast, the cells expressing DICER^{44ab} retained the decondensed state observed in unexposed shDICER cells suggesting that the catalytic function of DICER is essential for maintenance of heterochromatin in unchallenged cells (Figure 4F). However, upon exposure to UV light, we did not observe a shift towards a more condensed state in either wildtype or mutant DICER expressing cells. (Figures 3F, 4E and F). Thus both wildtype DICER and the inactive mutant were able to rescue the chromatin conformation phenotype of DICER knockdown cells in response to UV damage. This suggests that the catalytic activity of DICER might be dispensible for the observed conformational changes after UV irradiation. In order to evaluate whether the catalytic activity of DICER is essential for NER, we expressed mCherry-DICER or mCherry- DICER^{44ab} in MRC-5 cells, and performed a UDS assay. We found that expression of the enzymatically inactive DICER mutant did not have a detrimental effect on repair activity, as measured by UDS (Supplementary Figure S4C). These data together point towards a potential role of DICER in NER that is independent of its catalytic activity.

It has been previously reported that DDB2 facilitates decondensation of chromatin upon tethering to a chromatin array (26). Since DDB2, ZRF1 and DICER operate in the GG-NER pathway, we wanted to determine whether the decondensation mediated by DDB2 also occurs in a DICER dependent manner, and vice versa. To this end we performed an experiment to co-tether DDB2 with either DICER or ZRF1, followed by measuring the size of the array. Notably, we found that co-tethering of DDB2 leads to an increase in both the ZRF1 and DICER mediated decondensation (Figure 5A–D). This additive effect suggests that chromatin decondensation via DDB2 or DICER/ZRF1 is in fact initiated independently of each other. In order to substantiate this finding, we measured the array size of the DDB2 tethered chromatin array in control and DICER knockdown cells. We found that knockdown of DICER did not affect the DDB2 mediated chromatin decondensation (Supplementary Figure S5A). We additionally assayed the DICER mediated decondensation in control and DDB2 knockdown cells. We found that knockdown of DDB2 had no effect on the DICER mediated decondensation (Supple-

A

Protein name	Gene name	Molecular weight	Number of peptides
Endoribonuclease Dicer	DICER1	255	103
Zuotin-related factor 1	DNAJC2	77	20
SWI/SNF-related matrix-associated actin-dependent regulator of chromatin subfamily A member 5	SMARCA5	116.78	21
Poly [ADP-ribose] polymerase I	PARP1	113.08	11

B

Protein name	Gene name	Molecular weight	Number of peptides
Zuotin-related factor 1	DNAJC2	77	41
Endoribonuclease Dicer	DICER1	255	17
SWI/SNF-related matrix-associated actin-dependent regulator of chromatin subfamily A member 5	SMARCA5	116.78	18
Poly [ADP-ribose] polymerase I	PARP1	113.08	14

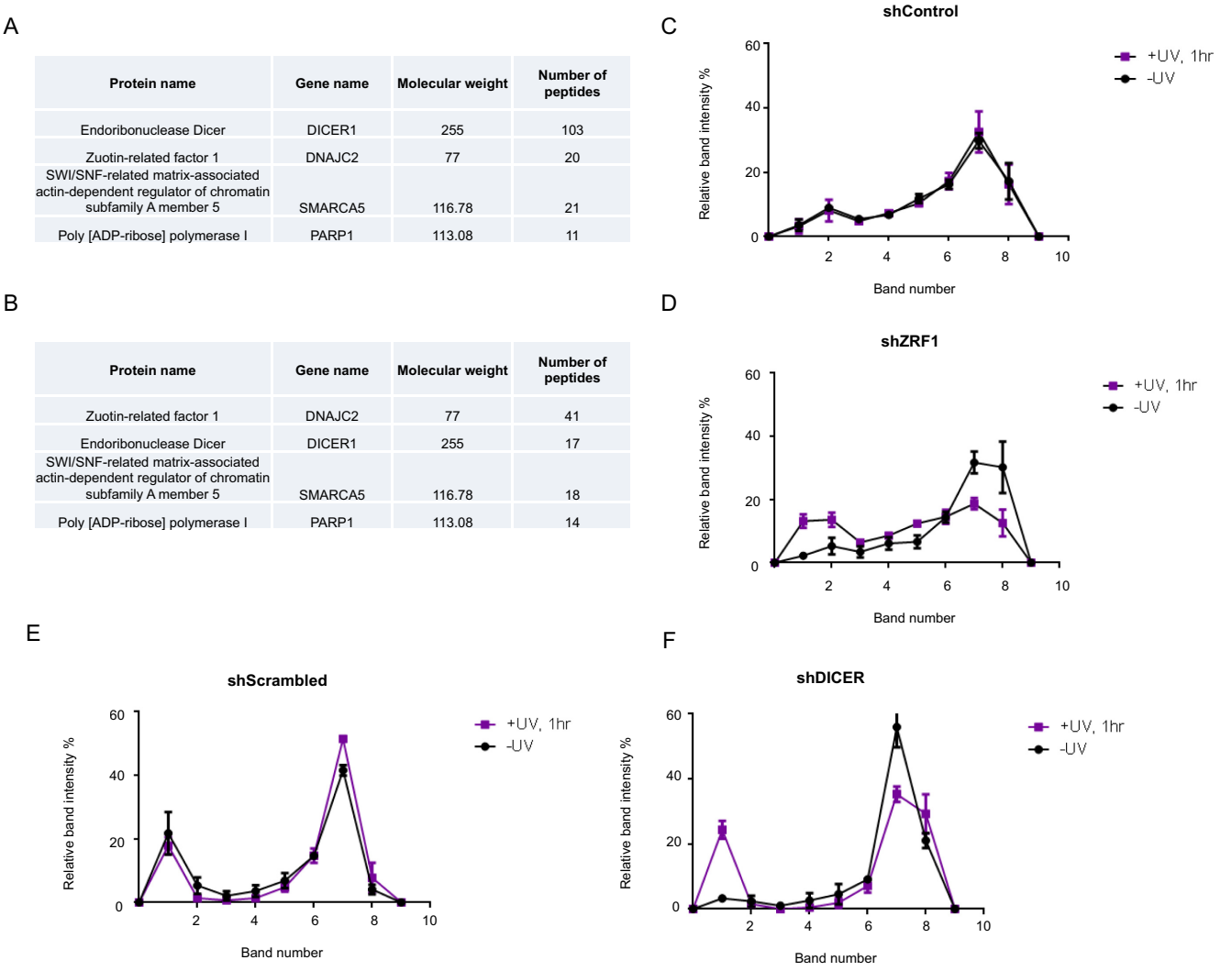

Figure 3. DICER and ZRF1 play a role in chromatin remodeling post UV exposure. (**A**, **B**) DICER and ZRF1 interact with various chromatin remodelers. $^{FLAG\text{-}HA}$DICER or ^{FLAG}ZRF1 along with its interactors, was purified from HEK293T cells and the purified material was subjected to mass spectrometry. Multiple proteins with chromatin remodeling functions were found to interact with DICER and ZRF1. The table shows peptide numbers for selected proteins obtained by affinity purification. (**C**–**F**) ZRF1 and DICER play a role in chromatin decondensation post UV exposure. Quantification of band intensities of MNAse digested chromatin from UV exposed cells in the indicated control and knockdown cells. Band numbers 1–8 depict DNA of high to low molecular weight. The graph shows the mean band intensity ±SD calculated from three independent experiments.

mentary Figure S5B) supporting that DICER and DDB2 might potentially contribute to decondensation of chromatin independently.

DICER and ZRF1 mediated decondensation requires PARP activity

Finally, we wanted to determine a potential mechanism by which ZRF1 and DICER might lead to decondensation of chromatin. It is well established that DDB2 decondenses chromatin in a PARP1-dependent manner (26) and that efficient NER requires parylation (3). In line with these findings and in agreement with our interaction data (Figure 3A and B), we examined whether ZRF1 and DICER mediated decondensation is also PARP dependent. To this end, we incubated DICER or ZRF1-LacR expressing cells with IPTG, followed by an IPTG release to enable chromatin binding of the LacR-fusion protein and treatment with a PARP inhibitor (KU-0058948). We subsequently fixed the cells after a 16 h incubation with PARP inhibitor and measured the array size. We found that inhibitor treatment reduced ZRF1 mediated chromatin decondensation (Figure 6A). Similarly, PARPi treatment also reduced DICER mediated chromatin decondensation (Figure 6B). In order to further confirm the role of PARP in the activity of ZRF1 and DICER, we measured the size of the ZRF1 or DICER tethered array in control and PARP1 knockdown cells. Similar to the effect of the PARP inhibitor, knockdown of PARP1 also significantly reduced the ability of ZRF1 and DICER to cause an increase in array size (Figure 6C). Next, we wanted to determine if the PARP1 mediated impact on the array size is also linked to UV damage repair. To this end, we treated HEK293T cells with either DMSO or

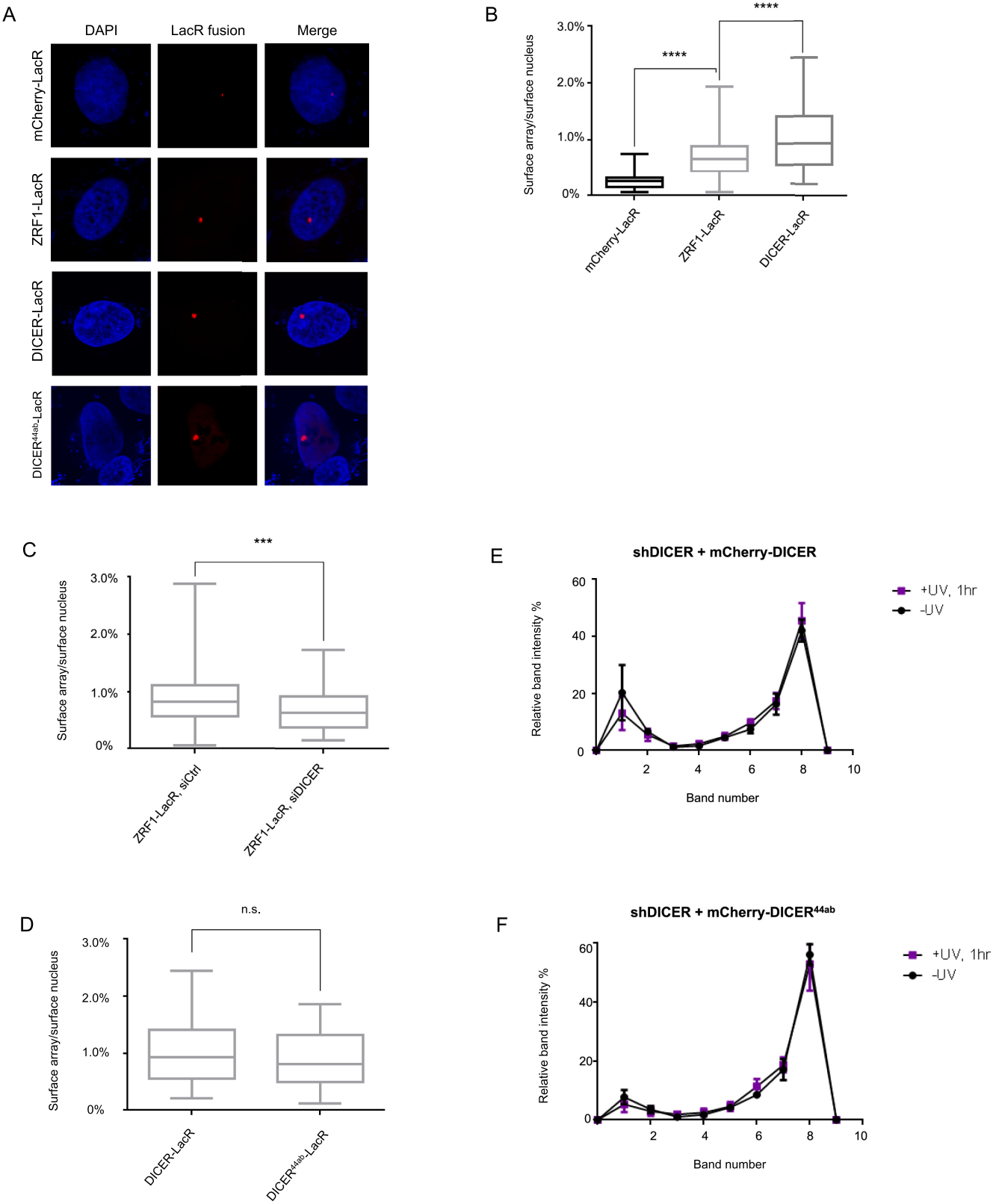

Figure 4. ZRF1 or DICER tethering facilitates decondensation of a chromatin array. (**A**) Representative immunofluorescence images showing the size of the LacO array after tethering of mCherry-LacR (control), ZRF1-LacR, DICER-LacR or DICER^{44ab}-LacR. (**B**–**D**) The graph shows the distribution (Min to Max) of percentage of nuclear area occupied by the specified tethered array in the specified knockdown conditions. Array size was measured in 50–100 cells from two independent experiments. Statistical significance was assessed by an unpaired *t*-test. (**E**, **F**) Quantification of band intensities of MNAse digested chromatin from UV exposed cells in shDICER cells expressing either wildtype or mutant DICER. Band numbers 1–8 depict DNA of high to low molecular weight. The graph shows the mean band intensity ±SD calculated from three independent experiments.

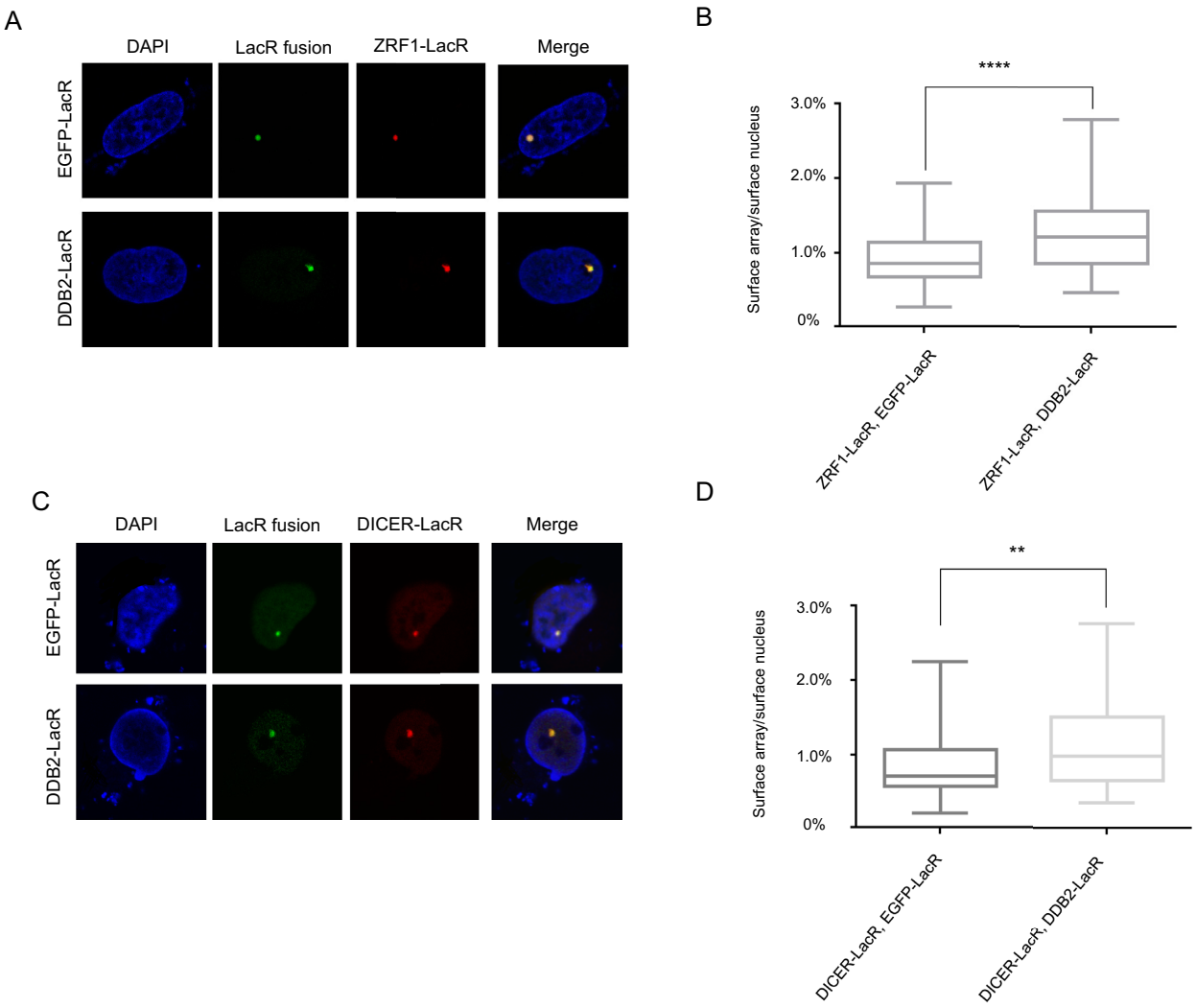

Figure 5. Co-tethering of ZRF1 or DICER with DDB2 increases array decondensation. (**A**, **C**) Representative images showing size of the LacO array after double tethering of mCherry-LacR-ZRF1 or mCherry-LacR-DICER with either EGFP-LacR (control) or EGFP-LacR-DDB2. (**B**, **D**) The graph shows the distribution (Min to Max) of percentage of nuclear area occupied by the specified tethered array. Array size was measured in 50–100 cells from two independent experiments. Statistical significance was assessed by an unpaired *t*-test.

PARPi and assessed the condensation state of chromatin before and after UV exposure. Similar to the effect observed for ZRF1 and DICER knockdown, treatment with PARP inhibitor also caused an increase in condensed chromatin in UV exposed cells. In contrast, administration of DMSO did not have any significant effect on the chromatin state (Figure 6D and E). Lastly, we directly assessed the effect of PARP1 depletion on UDS. We found that knockdown of PARP1 also reduced the repair dependent EdU incorporation after UV damage (Supplementary Figure S6A). Thus, PARP1 plays an important role in maintenance of chromatin state during NER.

In sum, our data provide evidence for a novel role of DICER in cooperation with ZRF1 and PARP1 in altering the chromatin conformation during nucleotide excision repair.

DISCUSSION

The endoribonuclease DICER is most well-known for its role in miRNA processing and RNAi mediated silencing via the RITS complex (21,44). Both these functions involve processing of RNAs by DICER to form short double-stranded RNA fragments. Additionally, DICER has also been shown to bind to rDNA (47). In this case, DICER was observed to bind to both active and inactive genes but its effect on the chromatin conformation remained uncertain. Furthermore, DICER was shown to operate at DSBs (16,17). Although the exact mechanism of dsRNAs produced by DICER in DSB repair stays elusive, it was recently reported that dsRNAs facilitate the recruitment of mediators of DNA damage signaling to chromatin (20). We assessed whether DICER also plays a role in other DNA damage pathways. Our data employing human cell lines and *C. elegans* unequivocally show that DICER is an essential player in NER. Reduction of DICER levels significantly re-

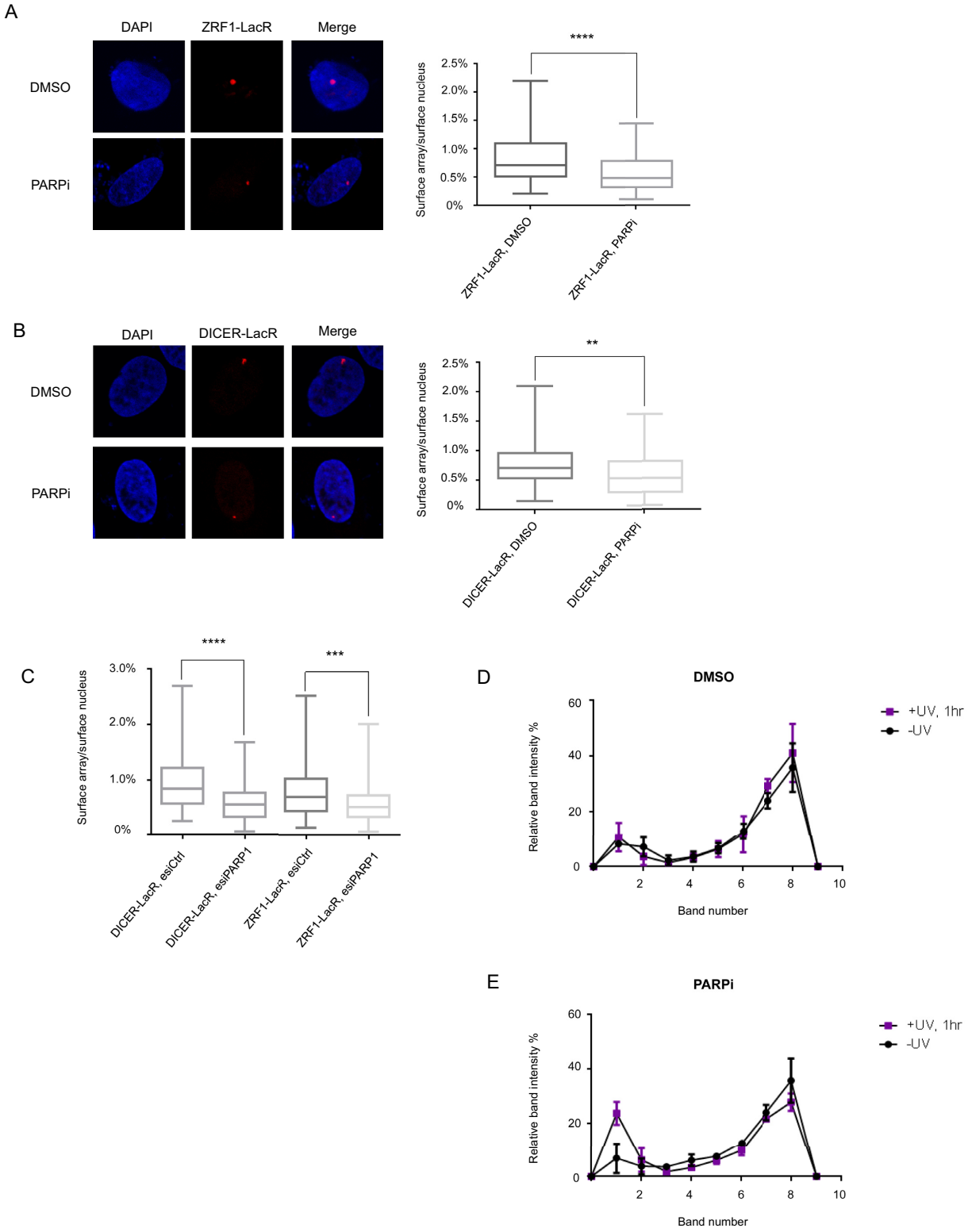

Figure 6. ZRF1 and DICER mediated decondensation is dependent on PARP. (**A**, **B**) (Left panel) Representative images showing the specified tethered array under specified treatment conditions. (Right panel) The graph shows the distribution (Min to Max) of percentage of nuclear area occupied by the specified tethered array, after treatment with vehicle (DMSO) or PARP inhibitor (PARPi). Array size was measured in 50–100 cells from two independent experiments. Statistical significance was assessed by an unpaired *t*-test. (**C**) The graph shows the distribution (Min to Max) of percentage of nuclear area occupied by the specified tethered array, after treatment in either control (esiControl) or PARP1 knockdown (esiPARP1) conditions. Array size was measured in 50–100 cells from two independent experiments. Statistical significance was assessed by an unpaired *t*-test. (**D**, **E**) Quantification of band intensities of MNAse digested chromatin from UV exposed cells in 293T cells treated with either DMSO or PARP inhibitor (PARPi). Band numbers 1–8 depict DNA of high to low molecular weight. The graph shows the mean band intensity ±SD calculated from three independent experiments.

duces the incorporation of EdU in UDS assays and UV irradiated dcr-1 strains show a severe germ line phenotype causing high mortality. In contrast, DICER depletion does not affect RRS, thus linking DICER preferentially to the GG-NER pathway. These findings are in agreement with the observed interaction of DICER and ZRF1, which is an important player in the GG-NER branch (12,15), and their localization to DNA damage sites.

Apart from its remodeling function at the DNA damage site (12), the H2A–ubiquitin binding protein ZRF1 is important for recruiting DICER to chromatin after UV irradiation. This further suggests that DICER is functionally linked to the ubiquitin signaling cascade during damage recognition. Interestingly, the binding of both proteins to chromatin seems to be RNA-dependent. In contrast, the interaction of both factors is not stabilized by RNA as judged by immunoprecipitation experiments involving RNAse digestion. Hence, RNA is probably not a scaffold for a putative protein complex consisting of ZRF1 and DICER but rather important for maintaining or recruiting these factors at chromatin. However, the exact role and nature of this RNA is still unclear.

Our mass spectroscopy experiments revealed a strong association of both ZRF1 and DICER with chromatin remodeling factors, and most notably with PARP1. In agreement with a potential function in chromatin remodeling, we observed a strong impact on the chromatin conformation after UV irradiation upon knockdown of ZRF1 or DICER. Likewise, when tethering both proteins to a genomic locus we observed a significant increase in size of the locus, implying a role in the decondensation of the locus. The decondensation seems to be carried out primarily by DICER, since knockdown of DICER also reduces the ZRF1 dependent decondensation. Hence, it appears that both proteins are involved in the decondensation of chromatin, which is an important prerequisite for DNA repair. ZRF1 had been linked to remodeling of protein complexes previously (12,15), however, here we provide evidence that it might play an additional role in chromatin remodeling during NER. DICER had been demonstrated to be involved in the formation of heterochromatin during gene silencing but whether it impacts on chromatin remodeling during DSB repair is still unknown. Here, we provide experimental evidence for a novel function of DICER which promotes the decondensation of chromatin. Consistent with their interaction with PARP1, ZRF1 and DICER mediated chromatin decondensation is entirely abolished when adding PARP inhibitors or when knocking down PARP1. This finding further substantiates potential functions of DICER and ZRF1 in chromatin remodeling. Interestingly, we found that DICER mediated chromatin decondensation is independent of its ribonuclease activity. Thus, even though the recruitment of DICER and ZRF1 to chromatin may potentially involve RNA, the decondensation activity likely does not.

Taken together our data highlight a novel and unexpected common role for ZRF1 and DICER during NER. DICER, apart from its catalytic function, harbors multiple domains that might be involved in recruitment of factors that drive the decondensation of chromatin. One potential candidate for such a function is evidently PARP1. Moreover, though speculative, the helicase activity of DICER might be involved in the decondensation process. Clearly, our study foreshadows also an RNA-independent chromatin remodeling function for DICER at DSBs, where the relationship of dsRNAs produced by DICER and its potential role in chromatin remodeling might be studied in more detail. Future research will certainly unveil the underlying molecular mechanisms.

SUPPLEMENTARY DATA

Supplementary Data are available at NAR Online.

ACKNOWLEDGEMENTS

We are grateful to the IMB microscopy facility for their expert help and assistance. We thank the members of the Richly laboratory for comments on the manuscript.

FUNDING

Boehringer Ingelheim Foundation; DFG [RI-2413/1-1]. Funding for open access charge: IMB.
Conflict of interest statement. None declared.

REFERENCES

1. de Laat,W.L., Jaspers,N.G. and Hoeijmakers,J.H. (1999) Molecular mechanism of nucleotide excision repair. *Genes Dev.*, **13**, 768–785.
2. Fousteri,M. and Mullenders,L.H. (2008) Transcription-coupled nucleotide excision repair in mammalian cells: molecular mechanisms and biological effects. *Cell Res.*, **18**, 73–84.
3. Marteijn,J.A., Lans,H., Vermeulen,W. and Hoeijmakers,J.H. (2014) Understanding nucleotide excision repair and its roles in cancer and ageing. *Nat. Rev. Mol. Cell Biol.*, **15**, 465–481.
4. Doil,C., Mailand,N., Bekker-Jensen,S., Menard,P., Larsen,D.H., Pepperkok,R., Ellenberg,J., Panier,S., Durocher,D., Bartek,J. *et al.* (2009) RNF168 binds and amplifies ubiquitin conjugates on damaged chromosomes to allow accumulation of repair proteins. *Cell*, **136**, 435–446.
5. Mattiroli,F., Vissers,J.H., van Dijk,W.J., Ikpa,P., Citterio,E., Vermeulen,W., Marteijn,J.A. and Sixma,T.K. (2012) RNF168 ubiquitinates K13-15 on H2A/H2AX to drive DNA damage signaling. *Cell*, **150**, 1182–1195.
6. Pan,M.R., Peng,G., Hung,W.C. and Lin,S.Y. (2011) Monoubiquitination of H2AX protein regulates DNA damage response signaling. *J. Biol. Chem.*, **286**, 28599–28607.
7. Ui,A., Nagaura,Y. and Yasui,A. (2015) Transcriptional elongation factor ENL phosphorylated by ATM recruits polycomb and switches off transcription for DSB repair. *Mol. Cell*, **58**, 468–482.
8. Bergink,S., Salomons,F.A., Hoogstraten,D., Groothuis,T.A., de Waard,H., Wu,J., Yuan,L., Citterio,E., Houtsmuller,A.B., Neefjes,J. *et al.* (2006) DNA damage triggers nucleotide excision repair-dependent monoubiquitylation of histone H2A. *Genes Dev.*, **20**, 1343–1352.
9. Kapetanaki,M.G., Guerrero-Santoro,J., Bisi,D.C., Hsieh,C.L., Rapic-Otrin,V. and Levine,A.S. (2006) The DDB1-CUL4ADDB2 ubiquitin ligase is deficient in xeroderma pigmentosum group E and targets histone H2A at UV-damaged DNA sites. *Proc. Natl. Acad. Sci. U.S.A.*, **103**, 2588–2593.
10. Marteijn,J.A., Bekker-Jensen,S., Mailand,N., Lans,H., Schwertman,P., Gourdin,A.M., Dantuma,N.P., Lukas,J. and Vermeulen,W. (2009) Nucleotide excision repair-induced H2A ubiquitination is dependent on MDC1 and RNF8 and reveals a universal DNA damage response. *J. Cell Biol.*, **186**, 835–847.
11. Guerrero-Santoro,J., Kapetanaki,M.G., Hsieh,C.L., Gorbachinsky,I., Levine,A.S. and Rapic-Otrin,V. (2008) The cullin 4B-based UV-damaged DNA-binding protein ligase binds to UV-damaged chromatin and ubiquitinates histone H2A. *Cancer Res.*, **68**, 5014–5022.

12. Gracheva,E., Chitale,S., Wilhelm,T., Rapp,A., Byrne,J., Stadler,J., Medina,R., Cardoso,M.C. and Richly,H. (2016) ZRF1 mediates remodeling of E3 ligases at DNA lesion sites during nucleotide excision repair. *J. Cell Biol.*, **213**, 185–200.
13. Riedl,T., Hanaoka,F. and Egly,J.M. (2003) The comings and goings of nucleotide excision repair factors on damaged DNA. *EMBO J.*, **22**, 5293–5303.
14. Sugasawa,K., Ng,J.M., Masutani,C., Iwai,S., van der Spek,P.J., Eker,A.P., Hanaoka,F., Bootsma,D. and Hoeijmakers,J.H. (1998) Xeroderma pigmentosum group C protein complex is the initiator of global genome nucleotide excision repair. *Mol. Cell*, **2**, 223–232.
15. Papadopoulou,T. and Richly,H. (2016) On-site remodeling at chromatin: How multiprotein complexes are rebuilt during DNA repair and transcriptional activation. *BioEssays*, **38**, 1130–1140.
16. Francia,S., Michelini,F., Saxena,A., Tang,D., de Hoon,M., Anelli,V., Mione,M., Carninci,P. and d'Adda di Fagagna,F. (2012) Site-specific DICER and DROSHA RNA products control the DNA-damage response. *Nature*, **488**, 231–235.
17. Wei,W., Ba,Z., Gao,M., Wu,Y., Ma,Y., Amiard,S., White,C.I., Rendtlew Danielsen,J.M., Yang,Y.G. and Qi,Y. (2012) A role for small RNAs in DNA double-strand break repair. *Cell*, **149**, 101–112.
18. Michalik,K.M., Bottcher,R. and Forstemann,K. (2012) A small RNA response at DNA ends in Drosophila. *Nucleic Acids Res.*, **40**, 9596–9603.
19. Gao,M., Wei,W., Li,M.M., Wu,Y.S., Ba,Z., Jin,K.X., Li,M.M., Liao,Y.Q., Adhikari,S., Chong,Z. *et al.* (2014) Ago2 facilitates Rad51 recruitment and DNA double-strand break repair by homologous recombination. *Cell Res.*, **24**, 532–541.
20. Francia,S., Cabrini,M., Matti,V., Oldani,A. and d'Adda di Fagagna,F. (2016) DICER, DROSHA and DNA damage response RNAs are necessary for the secondary recruitment of DNA damage response factors. *J. Cell Sci.*, **129**, 1468–1476.
21. Holoch,D. and Moazed,D. (2015) RNA-mediated epigenetic regulation of gene expression. *Nat. Rev. Genet.*, **16**, 71–84.
22. Jia,N., Nakazawa,Y., Guo,C., Shimada,M., Sethi,M., Takahashi,Y., Ueda,H., Nagayama,Y. and Ogi,T. (2015) A rapid, comprehensive system for assaying DNA repair activity and cytotoxic effects of DNA-damaging reagents. *Nat. Protoc.*, **10**, 12–24.
23. Craig,A.L., Moser,S.C., Bailly,A.P. and Gartner,A. (2012) Methods for studying the DNA damage response in the Caenorhabdatis elegans germ line. *Methods Cell Biol.*, **107**, 321–352.
24. Schmitter,D., Filkowski,J., Sewer,A., Pillai,R.S., Oakeley,E.J., Zavolan,M., Svoboda,P. and Filipowicz,W. (2006) Effects of Dicer and Argonaute down-regulation on mRNA levels in human HEK293 cells. *Nucleic Acids Res.*, **34**, 4801–4815.
25. Katsumi,S., Kobayashi,N., Imoto,K., Nakagawa,A., Yamashina,Y., Muramatsu,T., Shirai,T., Miyagawa,S., Sugiura,S., Hanaoka,F. *et al.* (2001) In situ visualization of ultraviolet-light-induced DNA damage repair in locally irradiated human fibroblasts. *J. Invest. Dermatol.*, **117**, 1156–1161.
26. Luijsterburg,M.S., Lindh,M., Acs,K., Vrouwe,M.G., Pines,A., van Attikum,H., Mullenders,L.H. and Dantuma,N.P. (2012) DDB2 promotes chromatin decondensation at UV-induced DNA damage. *J. Cell Biol.*, **197**, 267–281.
27. Richly,H., Rocha-Viegas,L., Ribeiro,J.D., Demajo,S., Gundem,G., Lopez-Bigas,N., Nakagawa,T., Rospert,S., Ito,T. and Di Croce,L. (2010) Transcriptional activation of polycomb-repressed genes by ZRF1. *Nature*, **468**, 1124–1128.
28. Bluhm,A., Casas-Vila,N., Scheibe,M. and Butter,F. (2015) Reader interactome of epigenetic histone marks in birds. *Proteomics*, **16**, 427–436.
29. Martini,E., Roche,D.M., Marheineke,K., Verreault,A. and Almouzni,G. (1998) Recruitment of phosphorylated chromatin assembly factor 1 to chromatin after UV irradiation of human cells. *J. Cell Biol.*, **143**, 563–575.
30. Maison,C., Bailly,D., Peters,A.H., Quivy,J.P., Roche,D., Taddei,A., Lachner,M., Jenuwein,T. and Almouzni,G. (2002) Higher-order structure in pericentric heterochromatin involves a distinct pattern of histone modification and an RNA component. *Nat. Genet.*, **30**, 329–334.
31. Zaret,K. (2005) Micrococcal nuclease analysis of chromatin structure. *Curr. Protoc. Mol. Biol.*, doi:10.1002/0471142727.mb2101s69.
32. Peng,J.C. and Karpen,G.H. (2009) Heterochromatic genome stability requires regulators of histone H3 K9 methylation. *PLoS Genet.*, **5**, e1000435.
33. Tang,K.F., Ren,H., Cao,J., Zeng,G.L., Xie,J., Chen,M., Wang,L. and He,C.X. (2008) Decreased Dicer expression elicits DNA damage and up-regulation of MICA and MICB. *J. Cell Biol.*, **182**, 233–239.
34. Mudhasani,R., Zhu,Z., Hutvagner,G., Eischen,C.M., Lyle,S., Hall,L.L., Lawrence,J.B., Imbalzano,A.N. and Jones,S.N. (2008) Loss of miRNA biogenesis induces p19Arf-p53 signaling and senescence in primary cells. *J. Cell Biol.*, **181**, 1055–1063.
35. Teta,M., Choi,Y.S., Okegbe,T., Wong,G., Tam,O.H., Chong,M.M., Seykora,J.T., Nagy,A., Littman,D.R., Andl,T. *et al.* (2012) Inducible deletion of epidermal Dicer and Drosha reveals multiple functions for miRNAs in postnatal skin. *Development*, **139**, 1405–1416.
36. Kraemer,A., Anastasov,N., Angermeier,M., Winkler,K., Atkinson,M.J. and Moertl,S. (2011) MicroRNA-mediated processes are essential for the cellular radiation response. *Radiat. Res.*, **176**, 575–586.
37. Pothof,J., Verkaik,N.S., van,I.W., Wiemer,E.A., Ta,V.T., van der Horst,G.T., Jaspers,N.G., van Gent,D.C., Hoeijmakers,J.H. and Persengiev,S.P. (2009) MicroRNA-mediated gene silencing modulates the UV-induced DNA-damage response. *EMBO J.*, **28**, 2090–2099.
38. Lans,H. and Vermeulen,W. (2015) Tissue specific response to DNA damage: C. elegans as role model. *DNA Repair (Amst.)*, **32**, 141–148.
39. Astin,J.W., O'Neil,N.J. and Kuwabara,P.E. (2008) Nucleotide excision repair and the degradation of RNA pol II by the Caenorhabditis elegans XPA and Rsp5 orthologues, RAD-3 and WWP-1. *DNA Repair (Amst.)*, **7**, 267–280.
40. Holoch,D. and Moazed,D. (2015) Small-RNA loading licenses Argonaute for assembly into a transcriptional silencing complex. *Nat. Struct. Mol. Biol.*, **22**, 328–335.
41. Papadopoulou,T., Kaymak,A., Sayols,S. and Richly,H. (2016) Dual role of Med12 in PRC1-dependent gene repression and ncRNA-mediated transcriptional activation. *Cell Cycle*, **15**, 1479–1493.
42. Robu,M., Shah,R.G., Petitclerc,N., Brind'Amour,J., Kandan-Kulangara,F. and Shah,G.M. (2013) Role of poly(ADP-ribose) polymerase-1 in the removal of UV-induced DNA lesions by nucleotide excision repair. *Proc. Natl. Acad. Sci. U.S.A.*, **110**, 1658–1663.
43. Janicki,S.M., Tsukamoto,T., Salghetti,S.E., Tansey,W.P., Sachidanandam,R., Prasanth,K.V., Ried,T., Shav-Tal,Y., Bertrand,E., Singer,R.H. *et al.* (2004) From silencing to gene expression: real-time analysis in single cells. *Cell*, **116**, 683–698.
44. Wilson,R.C. and Doudna,J.A. (2013) Molecular mechanisms of RNA interference. *Annu. Rev. Biophys.*, **42**, 217–239.
45. Wang,Q. and Goldstein,M. (2016) Small RNAs recruit chromatin-modifying enzymes MMSET and Tip60 to reconfigure damaged DNA upon double-strand break and facilitate repair. *Cancer Res.*, **76**, 1904–1915.
46. Zhang,H., Kolb,F.A., Jaskiewicz,L., Westhof,E. and Filipowicz,W. (2004) Single processing center models for human Dicer and bacterial RNase III. *Cell*, **118**, 57–68.
47. Sinkkonen,L., Hugenschmidt,T., Filipowicz,W. and Svoboda,P. (2010) Dicer is associated with ribosomal DNA chromatin in mammalian cells. *PLoS One*, **5**, e12175.